




Abnormalities of white and grey matter in early multiple system atrophy: comparison of parkinsonian and cerebellar variants

Santosh Kumar Dash¹ · Albert Stezin² · Tejashree Takalkar³ · Lija George¹ · Nitish L Kamble¹ · M Netravathi¹ · Ravi Yadav¹ · Keshav J. Kumar⁴ · Madhura Ingalhalikar³ · Jitender Saini⁵ · Pramod Kumar Pal¹ 

Received: 24 February 2018 / Revised: 21 May 2018 / Accepted: 5 June 2018 / Published online: 4 July 2018
© European Society of Radiology 2018

Abstract

Objective Multiple system atrophy (MSA) is a neurodegenerative disorder with progressive motor and autonomic dysfunction. There is a paucity of information on the early neurostructural changes in MSA, especially its subtypes, MSA-P (patients with predominant parkinsonism) and MSA-C (patients with predominant cerebellar signs). This study investigates the abnormalities of grey matter (GM) and white matter (WM) in early MSA and its subtypes using multi-modal voxel-based analysis.

Materials and methods Twenty-six patients with MSA with duration of symptoms ≤ 2.5 years (mean duration: 1.6 ± 0.9 years) were assessed clinically and with 3T MRI. Voxel-based morphometry (VBM) and diffusion tensor imaging (DTI) were performed to identify the structural changes in MSA and its subtypes. The GM changes and diffusion parameters of WM tracts were correlated with the clinical scores. The results were compared with MRI of 25 age- and gender-matched healthy controls.

Results The early structural changes in MSA included GM loss of the cerebellum and subcallosal gyrus with widespread involvement of supratentorial and infratentorial WM fibres. In MSA-C, GM loss was limited to the cerebellum with WM changes predominantly affecting the infratentorial WM and association tracts. In contrast, MSA-P did not demonstrate any GM loss and the WM involvement was mainly supratentorial. There was no significant correlation between structural changes and clinical severity score.

Conclusion In early MSA, WM microstructure was more affected than GM. These changes were greater in MSA-C than in MSA-P, suggesting variable deterioration in the subtypes of MSA.

Key Points

- Structural changes in early multiple system atrophy were evaluated using multi-modal neuroimaging.
- White matter was more affected than grey matter in early MSA.
- Clinical variables did not correlate with early structural changes.

Keywords Multiple system atrophy · Cerebellum · Neuroimaging · Diffusion tensor imaging

Santosh Kumar Dash and Albert Stezin contributed equally to this work.

Electronic supplementary material The online version of this article (<https://doi.org/10.1007/s00330-018-5594-9>) contains supplementary material, which is available to authorized users.

✉ Pramod Kumar Pal
palpramod@hotmail.com

¹ Department of Neurology, National Institute of Mental Health & Neurosciences, Hosur Road, Bangalore, Karnataka 560029, India

² Department of Clinical Neuroscience and Department of Neurology, National Institute of Mental Health & Neurosciences, Hosur Road, Bangalore, Karnataka 560029, India

³ Symbiosis Institute of Technology, Symbiosis International University, Lavale, Pune, India

⁴ Department of Clinical Psychology, National Institute of Mental Health and Neurosciences, Hosur Road, Bangalore, Karnataka 560029, India

⁵ Department of Neuroimaging & Interventional Radiology, National Institute of Mental Health & Neurosciences, Hosur Road, Bangalore, Karnataka 560029, India

Abbreviations

| | |
|----------|---|
| CC | Corpus callosum |
| DTI | Diffusion tensor imaging |
| EMSA-SG | European multiple system atrophy study group |
| FA | Fractional anisotropy |
| GM | Grey matter |
| IC | Internal capsule |
| ICP | Inferior cerebellar peduncle |
| IFOF | Inferior fronto-occipital fasciculus |
| MCP | Middle cerebellar peduncle |
| MD | Mean diffusivity |
| MRI | Magnetic resonance imaging |
| MSA-C | Cerebellar ataxia predominant multiple system atrophy |
| MSA-P | Parkinsonism predominant multiple system atrophy |
| MSA | Multiple system atrophy |
| NAMSA-SG | North American multiple system atrophy study group |
| SLF | Superior longitudinal fasciculus |
| UMSARS | Unified multiple system atrophy rating scale |
| VBM | Voxel-based morphometry |
| WM | White matter |

Introduction

Multiple system atrophy (MSA) is an adult-onset neurodegenerative disorder with a prevalence of 3.4–4.9 cases per a population of 100,000 and an estimated mean incidence of 0.6–0.7 cases per 100,000 person-years [1, 2]. During the course of its natural history, patients with MSA may manifest varying combinations of cerebellar ataxia, parkinsonism, autonomic failure and pyramidal involvement [3]. Based on the predominant motor symptomatology, MSA is classified into parkinsonism predominant MSA (MSA-P) and cerebellar ataxia predominant MSA (MSA-C) [4]. Neuro-pathologically, MSA is characterized by widespread neuronal loss and gliosis affecting the cerebellum, basal ganglia, pons, inferior olivary nuclei, and spinal cord [5]. Routine clinical MRI in MSA shows abnormalities such as volume loss and T2 hypo-intensity with marginal hyper-intensity of the putamen, atrophic changes of the brainstem, middle cerebellar peduncle (MCP), and the cerebellum [6]. Recently, advanced neuroimaging techniques have revealed loss of grey matter (GM) in the caudate, putamen, cerebellum, thalamus, hippocampus, insula, amygdala, parahippocampal gyrus, and fronto-temporal cortices, while the white matter (WM) abnormalities have been observed in the MCP, corticospinal tract, cerebellum, thalamic radiations, internal capsule, pons, corpus callosum, superior longitudinal fasciculus, and inferior cerebellar peduncle [7–21]. However,

these cohorts are demographically heterogeneous, consisting of patients with varying duration of disease and clinical severity. Hence, there is a lack of studies on the early structural changes in MSA. In a previous study, Oishi et al. [13] studied the WM changes in patients with MSA-C with short duration of disease (less than 2 years) and described diffusion changes restricted to the infra-tentorial regions. However, they did not perform whole-brain analysis and therefore their results do not provide information on the global WM changes in early MSA. Although many structural imaging studies have been performed on MSA, they have explored either GM or WM changes and did not investigate the multi-tissue abnormalities simultaneously in a specific cohort of patients, especially in early MSA [7–21]. Furthermore, information on the GM and WM change in subtypes of early MSA is also lacking. Studying the GM and WM changes and their distribution in early MSA may not only provide a better understanding of the disease biology, but also help identify robust biomarkers for early diagnosis of the disease, especially since research on disease-modifying agents in MSA are underway.

This study endeavours to identify the early neuro-structural abnormalities in MSA using multi-modal analysis involving voxel-based morphometry (VBM) and diffusion tensor imaging (DTI) in a large cohort of patients with MSA. For the purpose of this study, early MSA was defined as duration of disease ≤ 2.5 years [$\sim 25\%$ of the median survival based from the European (EMSA-SG) and North American MSA study groups (NAMSA-SG)] [22, 23].

Materials and methods

This study was conducted in the Department of Neurology and Department of Neuroimaging and Interventional Radiology (NIIR) at the National Institute of Mental Health and Neurosciences (NIMHANS), India. The study was scientifically and ethically approved by the institutional ethics committee and all subjects provided informed consent to participate in the study.

Subjects

Thirty subjects diagnosed as probable MSA based on the 2nd consensus criteria for MSA [4], with duration of disease ≤ 2.5 years from the onset of first motor symptom were recruited for the study. Patients with presence of other comorbid neurological disorders or contraindication for MRI were excluded. Twenty-five age- and gender-matched subjects without any neurological or psychiatric symptoms were recruited as controls.

Clinical details

The demographic and clinical details of patients were recorded systematically. Clinical evaluation was performed by

experienced neurologists, and patients with MSA were grouped into MSA-P and MSA-C based on the predominant clinical symptomatology. The Unified Multiple System Atrophy Rating Scale (UMSARS) part 2 and part 4 were used as the measure of severity of the disease.

Magnetic resonance imaging of the brain

MRI scans were acquired using 3-Tesla (T) Philips Achieva scanner (Philips Healthcare, Netherlands). Routine T2-weighted and fluid-attenuated inversion recovery (FLAIR) images were acquired followed by a high-resolution, three-dimensional T1 turbo field echo sequence covering the whole brain with repetition time (TR) = 8.1 milliseconds (ms), echo time (TE) = 3.7 ms, flip angle = 8°, sense factor = 3.5, voxel size = 1 × 1 × 1 millimetre (mm), acquisition matrix = 256 × 256, and total scan time = 7 min 41 s with 160 sagittal slices. DTI was performed by using single-shot spin-echo, echo-planar sequences in axial sections with the following settings: TR = 8783 ms, TE = 62 ms, flip angle = 8°, sense factor = 3.5, voxel size = 1.75 × 1.75 × 2 mm, acquisition matrix = 224 × 224 mm and 70 slices without any interslice gap. DTI was performed along 15 directions with a b value = 1000 s/mm² and NEX-2 with scan time of 5 min 35 sec. In addition, the images without diffusion weighting were acquired corresponding to b = 0 s/mm².

Voxel-based morphometry in MSA

VBM was used to detect the GM abnormalities from the T1 images. Data analysis was performed using the VBM8 toolbox in SPM8 software (available from <http://www.fil.ion.ucl.ac.uk/spm/>; Wellcome Trust Centre for Neuroimaging, London, UK) using MATLAB R2013a. The raw T1-weighted anatomical data in DICOM format were imported to SPM8 and saved as SPM-compatible NIFTI format. The images were spatially normalized by reorienting the T1-weighted anatomical images of all subjects into the same stereotactic space. These images were then segmented into GM, WM, cerebrospinal fluid (CSF), and non-CSF components. The segmented images subsequently underwent normalization to the Montreal Neurological Institute (MNI) space and modulation. The modulated images were smoothed using an 8-mm full-width half-maximum (FWHM) Gaussian kernel prior to statistical analysis. A two-sample *t* test was performed using age, duration of disease, and total intracranial volume (TIV) as covariates to investigate the differences between the two groups. Corrections for multiple comparisons were performed using the theory of Gaussian random fields and interpreted at a significance level of $p < 0.05$. The output from the procedure was a statistical parametric map depicting regions where GM concentrations varied significantly among the two groups. The MNI coordinates of these GM areas were

converted into Talairach coordinates using Ginger ALE (<http://www.brainmap.org/ale/>) and their anatomical location was obtained.

Diffusion tensor imaging in MSA

DTI was employed to detect WM changes. We used FSL 5.0.9 (available from <https://fsl.fmrib.ox.ac.uk/>) for pre-processing and for performing tract-based spatial statistics (TBSS). The pre-processing steps included conversion to NIFTI format, manual quality assessment to check for missing slices, visual assessment to identify intensity artifacts, and brain extraction using FSL's 'BET' [24]. Eddy current and motion correction was performed using FSL's 'eddycorrect' tool that employs an affine transformation between the baseline b = 0 image and the gradient images. Based on the rotation parameter in the affine transformation, the gradients were rotated using 'fdt_rotate_bvecs' to match the transformed images. To reduce the Rician noise in the DWI images, a joint linear minimum mean square error (jLMMSE) filter with default estimation and filtering radius was employed [25]. The diffusion tensor images were then reconstructed using least square approximations and manually checked to ensure that the tensors aligned with the underlying anatomy and no gradient flip were required. Finally, the scalar images of fractional anisotropy (FA) and mean diffusivity (MD) were obtained from the tensors.

Tract-based spatial statistics on diffusion MRI images

To analyse the changes in the WM in MSA, we performed TBSS on the FA and MD images derived from the diffusion MRI images. For TBSS, non-linear registration and alignment into one target image were performed. We chose one of the healthy controls with median brain volume as our target image. This target image was then affine-aligned into 1 × 1 × 1 mm MNI space. Using this transform, the FA images were aligned to the target FA image in MNI space to create a group mean FA image. The mean FA image was then used to obtain the WM skeleton, which represents the central path of all WM tracts and is common to the groups under consideration. A threshold of 0.2 was set to define set of voxels for binary skeleton mask and a distance map was formed to estimate FA over the skeleton mask. Once a 4-D FA skeletonized image was formed, voxel-wise statistics were performed with the null hypothesis of no significant differences between the two groups. A significance threshold of $p = 0.05$ was considered after performing non-parametric permutations testing with 5000 permutations to correct for multiple comparisons. For MD images, the wrap from non-linear registration of FA images was used to get MD images of all subjects aligned into one space. These MD images were merged into a 4-D MD image and then projected into mean FA skeleton image to get a 4-D skeletonized MD image. The voxel-wise cross-subject

statistics were performed on the raw t-stats image while using randomized 5000 permutations for multiple comparisons correction.

Clinical and neuroimaging correlations

Correlations were performed using the GM volume of atrophic areas (derived from VBM analysis), the mean FA, and MD values of statistically significant areas (derived from DTI-TBSS) with clinical scores such as scores of UMSARS-2, UMSARS-4, and duration of disease to assess the clinical correlates of neuro-anatomical correlates. The correlations were assessed at an FWE (family-wise error)-corrected threshold of $p < 0.05$, and only the significant ones were reported.

Results

Clinical

This study included 30 patients (13 women: 17 men) with probable MSA and 25 age- and gender-matched healthy controls. Based on the clinical symptoms and consensus by the investigating neurologists, 9 subjects were classified as MSA-P and 20 subjects were classified as MSA-C. One patient had mixed cerebellar and parkinsonian symptoms and was excluded from the analysis since a consensus could not be achieved. Furthermore, three MRI (one MSA-P and two MSA-C) were excluded due to movement artifacts. A total of 26 subjects and 25 control MRIs were included in the final analysis. The mean age at onset of symptom was 51.8 ± 5.9 years and the mean duration of disease was 1.6 ± 0.9 years. The mean UMSARS part 2 score of the overall cohort was 16.0 ± 8.2 and median UMSARS part 4 score was 2 (range 1–3). No significant difference was obtained in the clinical parameters among MSA subtypes (Tables 1 and 2).

Table 1 Demographic and clinical score in patients with multiple system atrophy and controls

| Demographic variable | MSA (n = 30) | MSA-C (n = 20) | MSA-P (n = 9) | Control (n = 25) | p value |
|-----------------------------|--------------|----------------|---------------|------------------|---------|
| Age (mean ±SD) | 54.4 ±5.86 | 55.7 ±5.4 | 53.8 ±6.0 | 55.0 ±6.8 | 0.74 |
| Gender (M/F) | 1.3:1 | 1:1 | 1.5:1 | 2.5:1 | 0.23 |
| Mean AAO (years) | 51.8 ±5.9 | 51 ±6.4 | 53.3 ±4.7 | – | 0.33 |
| Duration of disease (years) | 1.6 ±0.9 | 1.7 ±0.8 | 1.5 ±1.0 | – | 0.56 |
| UMSARS part 2 score | 16 ±8.2 | 16.9 ±9.6 | 16.8±7.7 | – | 0.92 |
| UMSARS part 4 score | 2 (1–3) | 2 (1–3) | 2 (1–3) | – | 1.0 |

AAO: age at onset, MSA: multiple system atrophy, MSA-C: multiple system atrophy-cerebellar phenotype, MSA-P: multiple system atrophy- parkinsonian phenotype, SD: standard deviation, UMSARS: Unified Multiple System Atrophy Rating Scale

Voxel-based morphometry in MSA

MSA vs. controls

In the overall cohort, clusters of GM loss were detected in the inferior semilunar lobule of the left cerebellum, left subcallosal gyrus, declive and the uvula of the right cerebellum ($p < 0.05$, FWE-corrected). In MSA-C, GM loss was present in the declive and pyramid of the right cerebellum, and bilateral uvula ($p < 0.05$, FWE-corrected. See Fig. 1). There was no significance in the MSA-P subjects compared to HCs.

MSA-C vs. MSA-P

There was no significant difference in the GM loss among the subtypes of MSA.

Correlation of clinical parameters and GM loss

No significant correlations were obtained when comparing the GM loss in the overall MSA cohort and in each subtype with duration of disease, UMSARS part 2, and UMSARS part 4 scores.

DTI-TBSS in MSA

MSA vs. controls The FA values were significantly reduced in the bilateral cerebellar WM, medial lemniscus, MCP, pontine fibres, midbrain, superior cerebellar peduncle (SCP), cerebral peduncles, the anterior and posterior limb of the internal capsule (IC), the superior longitudinal fasciculus (SLF), corpus callosum (CC), and fronto-occipital WM. ($p < 0.05$, few-corrected, Fig. 2). The MD values of bilateral cerebellar WM, middle cerebellar peduncle (MCP), pontine fibres, SCP, cerebral peduncles, posterior limb of th IC, inferior longitudinal fasciculus (ILF), SLF, inferior fronto-occipital fasciculus (IFOF), uncinate fasciculus, anterior limb of the IC, anterior thalamic radiation, CC, and frontal and occipital WM were significantly

Table 2 Areas of significant grey matter loss ($p < 0.05$, FWE-corrected) in MSA using voxel-based morphometry

| X | Y | Z | Peak equivalent | p value | Brain area | Grey matter area |
|---|--------|--------|-----------------|-----------|------------------|----------------------------|
| Grey matter atrophy in MSA compared to healthy controls | | | | | | |
| -21.59 | -72.45 | -36.73 | 4.82 | 0.003 | Left cerebellum | Inferior semi-lunar lobule |
| -28.55 | 8.33 | -11.63 | 4.72 | 0.003 | Left cerebrum | Subcallosal gyrus |
| 31 | -65.65 | -21.69 | 4.6 | 0.003 | Right cerebellum | Declive |
| 24.07 | -69.68 | -23.54 | 4.61 | 0.003 | Right cerebellum | Uvula |
| Grey matter atrophy in MSA-C compared to healthy controls | | | | | | |
| -20.32 | -69.18 | -26.94 | 5.28 | 0.0001 | Left cerebellum | Uvula |
| 6.05 | -70.72 | -26.64 | 4.66 | 0.0002 | Right cerebellum | Pyramid |
| -6.48 | -58.6 | -20.3 | 4.87 | 0.0002 | Left cerebellum | Fastigium |
| -6.57 | -68.9 | -15.87 | 4.72 | 0.0002 | Left cerebellum | Declive |

MSA: multiple system atrophy, MSA-C: multiple system atrophy-cerebellar phenotype, MSA-P: multiple system atrophy-parkinsonian phenotype, FWE: family-wise error. Comparison of MSA-P versus controls and MSA-C versus MSA-P did not provide significant grey matter loss

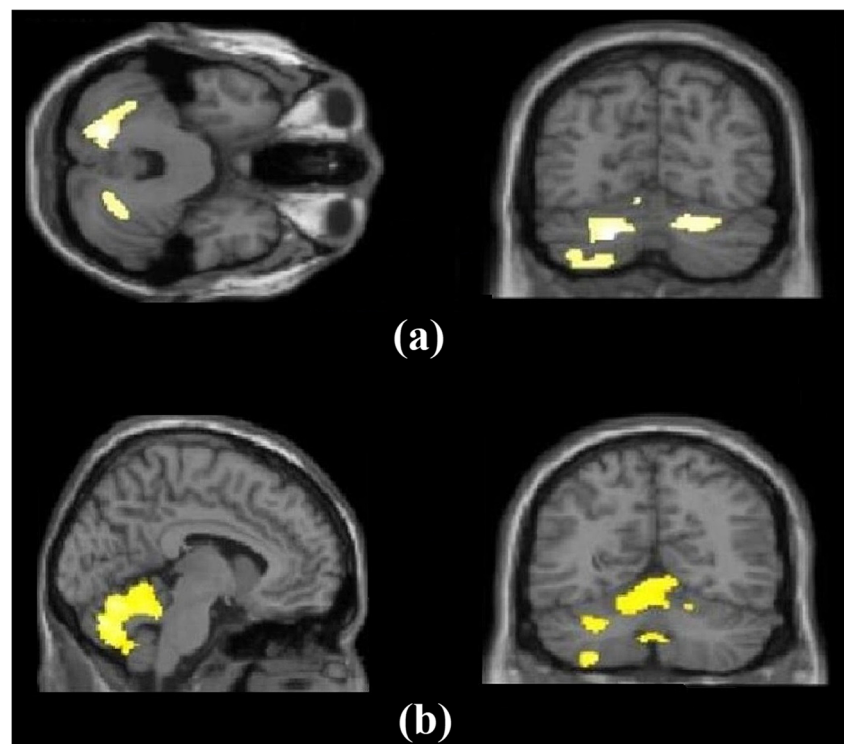
increased ($p < 0.05$, FWE-corrected, Fig. 2). Reverse contrast did not show any significant difference.

MSA-C vs. controls Significantly reduced FA values were noted in the MCP, ICP, corticospinal tract (CST), anterior and posterior limbs of the IC, body of CC, and cingulum in patients with MSA-C ($p < 0.05$, FWE-corrected). Increase in MD values was observed in the MCP, pontine crossing tract, CC, medial lemniscus, corona radiata, external capsule in MSA-C ($p < 0.05$, FWE-corrected).

MSA-P vs. controls Significantly reduced FA values were obtained in the anterior thalamic radiation, CST, and SLF in MSA-P ($p < 0.05$, FWE-corrected). Higher MD values were detected in the superior corona radiata and posterior limb of the IC ($p < 0.05$, FWE-corrected).

MSA-C vs. MSA-P On comparison with MSA-P, patients with MSA-C had reduced FA of the bilateral cerebellar WM, MCP, pontine fibres, SCP, midbrain, cerebral peduncles, the anterior and posterior limbs of the IC, left IFOF, uncinate fasciculus, left SLF, and frontal WM (p

Fig. 1 GM volume loss in MSA ($p < 0.05$, FWE-corrected): (a) MSA versus controls showing loss of grey matter volume in the inferior semilunar lobule of the left cerebellum, left subcallosal gyrus, declive, and the uvula of the right cerebellum; (b) MSA-C versus controls ($p < 0.05$, FWE-corrected) showing grey matter loss in the right declive and pyramid of right cerebellum, and bilateral uvula of cerebellum. No significant areas of grey matter loss were obtained between MSA-P versus controls and MSA-P versus MSA-C



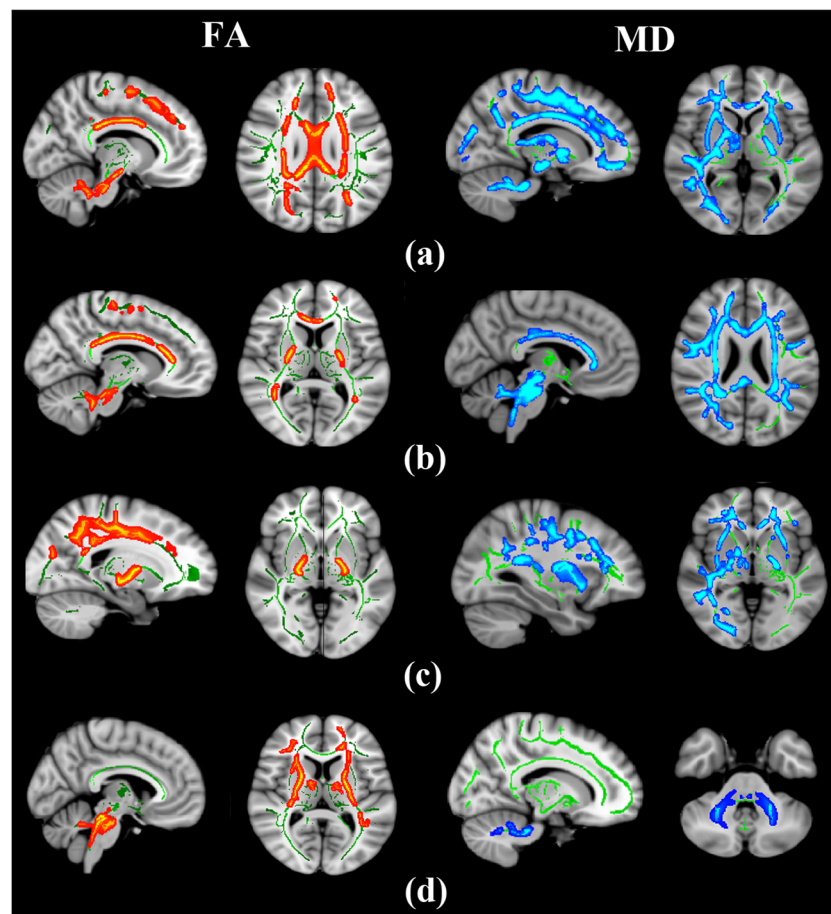


Fig. 2 WM diffusion changes in MSA ($p < 0.05$, FWE-corrected). **(a)** MSA versus controls. Decreased FA in bilateral cerebellar WM, medial lemniscus, middle cerebellar peduncle, pontine fibres, midbrain, superior cerebellar peduncle, cerebral peduncles, anterior and posterior limb of internal capsule, superior longitudinal fasciculus, corpus callosum and fronto-occipital WM. Increased MD in bilateral cerebellar WM, middle cerebellar peduncle, pontine fibres, superior cerebellar peduncle, cerebral peduncles, posterior limb of the internal capsule, inferior longitudinal fasciculus, superior longitudinal fasciculus, inferior fronto-occipital fasciculus, uncinate fasciculus, anterior limb of internal capsule, anterior thalamic radiation, corpus callosum, and frontal and occipital WM. Reverse contrast did not show any significant difference. **(b)** MSA-C versus controls. Reduced FA values were noted in middle cerebellar peduncle, inferior cerebellar peduncle, corticospinal tract, anterior and posterior limbs of the internal capsule, corpus callosum, and cingulum.

< 0.05 , FWE-corrected). MD was increased in the bilateral cerebellar WM, MCP, pontine fibres, and SCP in MSA-C ($p < 0.05$, FWE-corrected). There was no significant difference in FA and MD values of any tracts in MSA-P compared to MSA-C (see Fig. 2).

Correlation of clinical parameters and DTI changes No significant correlations (after correction for multiple comparisons) were obtained when comparing the FA and MD changes in the overall MSA cohort and in the subtypes with duration of disease, UMSARS part 2, and UMSARS part 4 score.

Increased MD values were noted in the middle cerebellar peduncle, pontine crossing tract, corpus callosum, medial lemniscus, corona radiata, and external capsule. **(c)** MSA-P versus controls. Reduced FA values were noted in the anterior thalamic radiation, corticospinal tract and superior longitudinal fasciculus. Increase in MD values were detected in the superior corona radiata and internal capsule. **(d)** MSA-C versus MSA-P. Decreased FA was noted in the bilateral cerebellar WM, middle cerebellar peduncle, pontine fibres, superior cerebellar peduncle, midbrain, cerebral peduncles, anterior and posterior limbs of the internal capsule, inferior fronto-occipital fasciculus, uncinate fasciculus, superior longitudinal fasciculus and frontal WM in MSA-C. MD was increased in the bilateral cerebellar WM, middle cerebellar peduncle, pontine fibres, and superior cerebellar peduncle in MSA-C. There was no significant difference in FA and MD values of any tracts in MSA-P compared to MSA-C

Discussion

This study performed multimodal analysis to identify the early structural changes in MSA. Our results demonstrate widespread WM involvement in comparison to GM loss in early MSA. On comparing the subtypes of MSA, MSA-C was detected to have more GM and WM involvement in comparison to MSA-P. No significant clinic-radiological correlations were obtained in this study.

Previous studies have reported GM volume loss in both supratentorial and infratentorial regions such as the cerebellum, pons, basal ganglia, thalamus, parts of the limbic system,

and fronto-temporal cortices in their cohorts. However, these cohorts have evaluated subjects with more advanced disease having longer mean duration of disease [7–21]. This study, in contrast, evaluated subjects with early MSA and identified cerebellar GM to be involved early in the disease process without the involvement of any other regions. In a study by Oishi et al. [13] on patients with pre-diagnostic and early MSA-C, GM changes were absent. A cursory analysis suggests that GM changes are a late feature in MSA.

In contrast to the GM changes, we demonstrate that WM changes are more confluent and involve both the supratentorial and infratentorial WM projections, commissural and association fibres, even in early MSA. Such widespread WM involvement is also reported in studies with longer duration of disease [7–21]. WM changes in early MSA-C was reported by Oishi et al. [13]. They demonstrated FA changes in the infratentorial structures such as the ventral pons, MCP, and ICP in MSA with progressive worsening of FA values in the advanced disease. However, being a region of interest (ROI) analysis, they did not report any supratentorial changes. No other advanced structural imaging studies have been performed in early MSA-P. However, a qualitative assessment of clinical MRI images in pre-diagnostic MSA-P by Mestre et al. revealed involvement of the putamen, cerebellum, MCP, and pons [26]. The structural changes obtained in this study endorse earlier findings and also establish original evidence suggesting widespread WM microstructural deficits in comparison to the limited GM atrophy in early MSA. Recent studies have hypothesized MSA to be an oligodendroglial synucleinopathy with "prion-like" propagation of misfolded α -synuclein from neurons to oligodendroglia and cell to cell [27] and therefore more likely to affect the WM more severely than GM. The widespread WM changes in early MSA compared to GM loss obtained in this study supports this hypothesis.

In this study, the comparison of early structural changes in MSA-C and MSA-P revealed GM volume loss and WM involvement to be more in MSA-C. When compared to controls, MSA-P had WM involvement of association tracts without any infratentorial involvement. On the other hand, patients with MSA-C demonstrated widespread WM changes both in supratentorial and infratentorial regions on comparison to controls. Comparison of MSA-C and MSA-P demonstrated structural changes in MSA-C to involve the WM of the cerebellum, hindbrain structures, and few association tracts. Our findings are supported by clinical neuroimaging studies which have demonstrated MSA-C to have more brain abnormalities, such as cerebellar and pontine involvement, compared to MSA-P [28]. However, in contrast, studies have not observed significant DTI changes (in FA and MD values) to differentiate subtypes of MSA [15, 19, 21]. The comparative structural changes in MSA subtypes, despite a similar duration of disease and age at onset, probably suggest a difference in the rate of

disease progression between MSA-C and MSA-P, at least in the early stages of the disease. However, previous studies have reported the natural history of MSA-C and MSA-P to be similar and therefore our observation must be interpreted with caution, especially since the sample size of MSA-P in our cohort was low [22, 23].

Interestingly, no significant correlations were observed between structural changes and clinical parameters such as duration of disease and scores of UMSARS part 2 and part 4 in MSA and its subgroups. Previous ROI-based DTI studies have consistently reported the clinical severity scores to be associated with WM changes of the cerebellum, MCP, and corticospinal tracts [29, 30]. In contrast, the correlation of clinical scores and GM atrophy were variable in different studies [8–13]. The absence of association between the clinical and neuroimaging changes may be related to the lesser severity and shorter duration of symptoms in our cohort of patients.

This study has a few strengths and limitations. Being a relatively uncommon disease, the sample size in previous studies was limited and consisted of patients with varying durations of illness. In this study, we recruited a larger, overall cohort size of subjects with early MSA. The median cohort size in the previous studies was 15.5 patients which further decreased to 14 subjects in MSA-C and 12.5 subjects in MSA-P when the subtypes were examined separately. The largest sample size of MSA-C was 32 subjects and MSA-P was 16 [31–38], (Supplementary Table 1). Despite being comparable, the sample size of subtypes of MSA, specifically MSA-P, in this study was small. Hence, the results are to be interpreted with caution. To get a better understanding of the changes in early MSA, we have recruited and evaluated a comparatively larger number of patients with shorter duration of disease. By utilizing VBM and DTI-TBSS concurrently in the same cohort of subjects, we have provided information on the extent and distribution of GM and WM changes and their differential involvement in early MSA.

Although we have met the principal objective that we set during the conceptualization of this study, some possible drawbacks should be taken into account. Consequent to the absence of large studies on the natural history of MSA from the Indian subcontinent, early MSA was defined based on the median survival data from the natural history of MSA studies from European and American cohorts despite the differences in the demographic profile of patients in our cohort. In addition, there is also a need to validate our findings in larger cohorts.

In summary, this study demonstrates the early structural changes in MSA and its subtypes. Our results show that WM involvement is comparatively more than GM loss in early MSA and involves the projection, association, and commissural fibre tracts. Among the subtypes of MSA, MSA-C seems to have more florid WM and GM changes compared to MSA-P, probably suggesting a faster progression of the

disease. However, larger studies on patients with different stages of MSA are required to confirm these findings.

Compliance with ethical standards

Guarantor The scientific guarantor of this publication is Dr. Pramod Kumar Pal.

Conflict of interest The authors of this manuscript declare no relationships with any companies whose products or services may be related to the subject matter of the article.

Financial disclosure The authors report no financial interests or conflicts of interest.

Statistics and biometry No complex statistical methods were necessary for this paper.

Informed consent Written informed consent was obtained from all subjects in this study.

Ethical approval Institutional review board approval was obtained.

Methodology

- prospective
- case-control study
- performed at one institution

References

1. Fanciulli A, Wenning GK (2015) Multiple-System Atrophy. *N Engl J Med* 372:249–263. <https://doi.org/10.1056/NEJMra1311488>
2. Stefanova N, Bücke P, Duerr S, Wenning GK (2009) Multiple system atrophy: an update. *Lancet Neurol*. 8:1172–1178
3. Wenning GK, Ben-Shlomo Y, Hughes A et al (2000) What clinical features are most useful to distinguish definite multiple system atrophy from Parkinson's disease? *J Neurol Neurosurg Psychiatry* 68: 434–440. <https://doi.org/10.1136/jnnp.68.4.434>
4. Gilman S, Wenning GK, Low PA et al (2008) Second consensus statement on the diagnosis of multiple system atrophy. *Neurology* 71:670–676. <https://doi.org/10.1212/01.wnl.0000324625.00404.15>
5. Ubhi K, Low P, Masliah E (2011) Multiple system atrophy: A clinical and neuropathological perspective. *Trends Neurosci* 34: 581–590. <https://doi.org/10.1016/j.tins.2011.08.003>
6. Brooks DJ, Seppi K (2009) Proposed neuroimaging criteria for the diagnosis of multiple system atrophy. *Mov Disord* 24:949–964. <https://doi.org/10.1002/mds.22413>
7. Kim H-J, Jeon BS, Kim YE et al (2013) Clinical and imaging characteristics of dementia in multiple system atrophy. *Parkinsonism Relat Disord* 19:617–21. doi: <https://doi.org/10.1016/j.parkreldis.2013.02.012>
8. Brenneis C, Boesch SM, Egger KE et al (2006) Cortical atrophy in the cerebellar variant of multiple system atrophy: A voxel-based morphometry study. *Mov Disord* 21:159–165. <https://doi.org/10.1002/mds.20656>
9. Chang CC, Chang YY, Chang WN et al (2009) Cognitive deficits in multiple system atrophy correlate with frontal atrophy and disease duration. *Eur J Neurol* 16:1144–1150. <https://doi.org/10.1111/j.1468-1331.2009.02661.x>
10. Tzarouchi LC, Astrakas LG, Konitsiotis S et al (2010) Voxel-based morphometry and voxel-based relaxometry in parkinsonian variant of multiple system atrophy. *J Neuroimaging* 20:260–266. <https://doi.org/10.1111/j.1552-6569.2008.00343.x>
11. Hauser T-K, Luft A, Skalej M et al (2006) Visualization and quantification of disease progression in multiple system atrophy. *Mov Disord* 21:1674–1681. <https://doi.org/10.1002/mds.21032>
12. Lee MJ, Shin J-H, Seoung J-K et al (2016) Cognitive impairments associated with morphological changes in cortical and subcortical structures in multiple system atrophy of the cerebellar type. *Eur J Neurol* 23:92–100. <https://doi.org/10.1111/ene.12796>
13. Oishi K, Konishi J, Mori S et al (2009) Reduced fractional anisotropy in early-stage cerebellar variant of multiple system atrophy. *J Neuroimaging* 19:127–131. <https://doi.org/10.1111/j.1552-6569.2008.00262.x>
14. Zanigni S, Evangelisti S, Testa C et al (2017) White matter and cortical changes in atypical parkinsonisms: A multimodal quantitative MR study. *Parkinsonism Relat Disord* 39:44–51. <https://doi.org/10.1016/j.parkreldis.2017.03.001>
15. Wang J, Wai Y, Lin W-Y et al (2010) Microstructural changes in patients with progressive supranuclear palsy: a diffusion tensor imaging study. *J Magn Reson Imaging* 32:69–75. <https://doi.org/10.1002/jmri.22229>
16. Blain CRV, Barker GJ, Jarosz JM et al (2006) Measuring brain stem and cerebellar damage in parkinsonian syndromes using diffusion tensor MRI. *Neurology* 67:2199–2205. <https://doi.org/10.1212/01.wnl.0000249307.59950.f8>
17. Wang PS, Wu HM, Lin CP, Soong BW (2011) Use of diffusion tensor imaging to identify similarities and differences between cerebellar and Parkinsonism forms of multiple system atrophy. *Neuroradiology* 53:471–481. <https://doi.org/10.1007/s00234-010-0757-7>
18. Wang P-S, Yeh C-L, Lu C-F et al (2016) The involvement of supratentorial white matter in multiple system atrophy: a diffusion tensor imaging tractography study. *Acta Neurol Belg* 117:213–220. <https://doi.org/10.1007/s13760-016-0724-0>
19. Ji L, Zhu D, Xiao C, Shi J (2014) Tract based spatial statistics in multiple system atrophy: A comparison between clinical subtypes. *Parkinsonism Relat Disord* 20:1050–1055. <https://doi.org/10.1016/j.parkreldis.2014.06.017>
20. Ito S, Makino T, Shirai W, Hattori T (2008) Diffusion tensor analysis of corpus callosum in progressive supranuclear palsy. *Neuroradiology* 50:981–985. <https://doi.org/10.1007/s00234-008-0447-x>
21. Rulseh AM, Keller J, Ruzs J et al (2016) Diffusion tensor imaging in the characterization of multiple system atrophy. *Neuropsychiatr Dis Treat* 12:2181–2187. <https://doi.org/10.2147/NDT.S109094>
22. Wenning GK, Geser F, Krismer F et al (2013) The natural history of multiple system atrophy: A prospective European cohort study. *Lancet Neurol*. 12:264–274. [https://doi.org/10.1016/S1474-4422\(12\)70327-7](https://doi.org/10.1016/S1474-4422(12)70327-7)
23. Low PA, Reich SG, Jankovic J et al (2015) Natural history of multiple system atrophy in the USA: a prospective cohort study. *Lancet Neurol*. 14:710–719. [https://doi.org/10.1016/s1474-4422\(15\)00058-7](https://doi.org/10.1016/s1474-4422(15)00058-7)
24. Popescu V, Battaglini M, Hoogstrate WS et al (2012) Optimizing parameter choice for FSL-Brain Extraction Tool (BET) on 3D T1 images in multiple sclerosis. *Neuroimage* 61:1484–1494. <https://doi.org/10.1016/j.neuroimage.2012.03.074>
25. Tristán-Vega A, Aja-Fernández S (2010) DWI filtering using joint information for DTI and HARDI. *Med Image Anal*. 14:205–218. <https://doi.org/10.1016/j.media.2009.11.001>
26. Mestre TA, Gupta A, Lang A E (2016) MRI signs of multiple system atrophy preceding the clinical diagnosis: the case for an imaging-supported probable MSA diagnostic category. *J Neurol Neurosurg Psychiatry*. 87 443–4.

27. Laurens B, Vergnet S, Lopez MC et al (2017) Multiple System Atrophy - State of the Art. *Curr Neurol Neurosci Rep* 17. <https://doi.org/10.1007/s11910-017-0751-0>
28. Roncevic D, Palma JA, Martinez J et al (2014) Cerebellar and parkinsonian phenotypes in multiple system atrophy: similarities, differences and survival. *J Neural Transm (Vienna)*. 121:507–512
29. Worker A, Blain C, Jarosz J et al (2014) Diffusion Tensor Imaging of Parkinson's Disease, Multiple System Atrophy and Progressive Supranuclear Palsy: A Tract-Based Spatial Statistics Study. *PLoS One*. 9:e112638. <https://doi.org/10.1371/journal.pone.0112638>
30. Tha KK, Terae S, Yabe I et al (2010) Microstructural white matter abnormalities of multiple system atrophy: in vivo topographic illustration by using diffusion-tensor MR imaging. *Radiology*. 255:563–569. <https://doi.org/10.1148/radiol.10090988>
31. Tir M, Delmaire C, Le Thuc V et al (2009) Motor-related circuit dysfunction in MSA-P: Usefulness of combined whole-brain imaging analysis. *Mov Disord* 24:863–870
32. Kim JS, Yang JJ, Lee DK et al (2015) Cognitive impairment and its structural correlates in the parkinsonian subtype of multiple system atrophy. *Neurodegener Dis* 15:294–300. <https://doi.org/10.1159/000430953>
33. Shigemoto Y, Matsuda H, Kamiya K et al (2013) In vivo evaluation of gray and white matter volume loss in the parkinsonian variant of multiple system atrophy using SPM8 plus DARTEL for VBM. *NeuroImage Clin* 2:491–496. <https://doi.org/10.1016/j.nicl.2013.03.017>
34. Minnerop M, Specht K, Ruhlmann J et al (2007) Voxel-based morphometry and voxel-based relaxometry in multiple system atrophy-A comparison between clinical subtypes and correlations with clinical parameters. *Neuroimage*. 36:1086–1095. <https://doi.org/10.1016/j.neuroimage.2007.04.028>
35. Minnerop M, Lüders E, Specht K et al (2010) Callosal tissue loss in multiple system atrophy-A one-year follow-up study. *Mov Disord* 25:2613–2620. <https://doi.org/10.1002/mds.23318>
36. Specht K, Minnerop M, Müller-Hübenthal J et al (2005) Complementary results by combining voxel-based morphometry and voxel-based relaxometry. *Neuroimage*. 25:287–293. <https://doi.org/10.1016/j.neuroimage.2004.11.022>
37. Brenneis C, Egger K, Scherfler C et al (2007) Progression of brain atrophy in multiple system atrophy: A longitudinal VBM study. *J Neurol* 254:191–196. <https://doi.org/10.1007/s00415-006-0325-6>
38. Yang H, Wang X, Liao W et al (2015) Application of diffusion tensor imaging in multiple system atrophy: the involvement of pontine transverse and longitudinal fibers. *Int J Neurosci* 125: 18–24.